Electrostatic forces and the frequency spectrum of a monolayer solid of linear molecules on graphite

Hansen, Flemming Yssing; Bruch, Ludwig Walter; Roosevelt, S. E.

Published in:
Physical Review B

Link to article, DOI:
10.1103/PhysRevB.45.11238

Publication date:
1992

Document Version
Publisher's PDF, also known as Version of record

Electrostatic forces and the frequency spectrum of a monolayer solid of linear molecules on graphite

F. Y. Hansen
Fysisk-Kemisk Institut, The Technical University of Denmark, DTH 206, DK-2800 Lyngby, Denmark

L. W. Bruch
Fysisk-Kemisk Institut, The Technical University of Denmark, DTH 206, DK-2800 Lyngby, Denmark
and Department of Physics, University of Wisconsin–Madison, Madison, Wisconsin 53706

S. E. Roosevelt
Department of Mathematics, Texas A&M University, College Station, Texas 77843
(Received 15 October 1991)

Electrostatic energies which arise from aspherical atomic charge distributions in a graphite substrate are included in the modeling of a commensurate molecular monolayer. For the planar (two-in) herringbone lattice of nitrogen on graphite such terms may resolve a discrepancy with experimental data for the Brillouin-zone-center frequency gap. The treatment includes consideration of a generalized (two-out) herringbone lattice and of the screening by the graphite of electrostatic fields from the multipole moments of adsorbed molecules. A small adjustment to a previous approximation for the latter process leads to stable modeling of the commensurate monolayer solid of carbon monoxide on graphite.

I. INTRODUCTION

Inelastic neutron-scattering experiments[1,2] have produced a measure of the dynamics of a commensurate monolayer solid, namely the Brillouin-zone-center frequency gap for in-plane vibrations with zero wave vector. The gap reflects the restoring force constant for lateral displacements of the center of mass of the monolayer, and it is related to the potential energy of the corrugation of the substrate surface.[3] Data were obtained[1,2] for the low-temperature orientationally ordered commensurate lattice of molecular nitrogen adsorbed on the basal-plane surface of graphite, which has been the subject of extensive modeling.[4,5] Models which reproduce many of the structural and energetic properties of the nitrogen monolayer and the high-frequency components of the observed spectrum gave minimum frequencies which are only half of the lowest observed frequency.[1] The discrepancy has persisted[3] in spite of several adjustments to the model of the molecule-to-graphite potential energy; such a large error suggests a serious failing in the characterization of this potential energy. We show here that electrostatic interactions arising[6,7] from aspherical charge distributions at the graphite atomic sites may suffice to remove the discrepancy. A discussion is included of the modeling[8,9] of electrostatic energies in the monolayer solid of carbon monoxide adsorbed on graphite, where such energies have a larger effect than for nitrogen.

Vernov and Steele,[6] extending a suggestion of Nicholson, Cracknell, and Parsonage[7] proposed that the carbon atoms in graphite have charge distortions which can be represented as local quadrupole moments and that the fields from the moments increase the corrugation of the interaction energy for adsorbed molecules with permanent electrostatic moments. Such a mechanism would not act for adsorbed inert gases; thus, discrepancies for modeling with parameters from the inert-gas series might have been anticipated. Vernov and Steele[6] used quadrupole moments for aromatic molecules to estimate an effective quadrupole moment for a bonded carbon atom. Earlier, Joshi and Tildesley[10] adjusted anisotropy parameters[11] in a van der Waals model of the molecule-to-graphite interaction to increase calculated barriers to lateral motion of the molecules.

We determine the structure and frequency spectrum of the commensurate $\sqrt{3}\times 3$ monolayer herringbone solid of nitrogen on graphite for several models with substrate quadrupole fields. As described in Sec. III, models with the (negative) quadrupole moment sign adopted by Vernov and Steele[6] lead to a class of generalized two-out herringbone lattices. There is a frustration of competing processes in the total potential energy and the lowest frequencies are even smaller than those for models without the quadrupoles. However, the graphite charge distribution derived from x-ray-diffraction data[12] leads to models with a positive sign of the effective quadrupole moment and a magnitude in a range which will reproduce the observed minimum frequency. The lattice spectral density at intermediate and high frequencies is affected little by the addition of this term, and the corrugation is increased in the sense required by Joshi and Tildesley[10] to bring their calculated monolayer melting temperatures into agreement with experiment.

Because our proposed resolution of the discrepancy in the zone-center frequency gap for nitrogen on graphite involves enhancing electrostatic terms in the potential energy, we examine the consequences of adding such terms to models[8] for carbon monoxide on graphite. Carbon monoxide and molecular nitrogen are treated[8] as closely related adsorbates: The van der Waals terms in the interaction are taken to be the same, but carbon monoxide has a permanent dipole moment and a larger quadrupole

moment than nitrogen. However, with a simple approximation[13] for screening of external electrostatic fields from the graphite, image energy terms are a perturbation for nitrogen, but are disastrously large for carbon monoxide.[8,9] We find that a small adjustment to the approximation for the screening is enough to stabilize the calculation for carbon monoxide, without much change in the results for nitrogen. The additional substrate electrostatic fields have a similar effect for carbon monoxide as for nitrogen. The commensurate two-out herringbone lattice was proposed by Belak, Kobashi, and Etters[8] to be a possible structure for adsorbed carbon monoxide.

We formulate and apply a version of the Born-Oppenheimer approximation for the frequency of center-of-mass oscillations.[3] The potential energy of the monolayer solid is calculated as a function of the position of the center of mass and force constants are derived from the curvature of the energy surface at the minimum position. Thus, estimates of the minimum frequency are obtained from results of multiparameter static potential-energy minimizations. In all the (nitrogen) cases for which we have lattice-dynamics results for the frequency spectrum, the approximation reproduces the lowest frequency to 10%. We use it to estimate the lowest frequency of a commensurate orientationally ordered monolayer carbon monoxide on graphite.

The organization of this paper is as follows. Section II contains the formulation of the calculations and a summary of the interaction models and the coordinates in the monolayer unit cell. Sections III and IV contain results for the modeling of nitrogen on graphite and carbon monoxide on graphite, respectively. Section V contains concluding remarks. Appendix A outlines the derivation of the Born-Oppenheimer approximation for center-of-mass oscillations, and Appendix B summarizes the argument for adjusting the position of the electrostatic screening mirror plane.

II. FORMULATION OF THE CALCULATIONS

The diatomic molecules N_2 and CO are assumed to be rigid, with fixed internuclear distance, and are described by five spatial coordinates. Our emphasis is on the structure and frequency spectrum of commensurate herringbone cells with two molecules per unit cell. We do not treat the stability of the minimum-energy configuration in the class of generalized herringbone lattices relative to commensurate lattices with more molecules per unit cell or relative to incommensurate lattices. For N_2, the modifications to the molecule-graphite potential generally increase the corrugation; earlier work with less-corrugated potentials had shown the herringbone lattice to be the ground state.[4,5] For CO, the corrugation is also increased; the stability analysis of Belak, Kobashi, and Etters[8] is discussed in Sec. IV.

A. Interaction models

1. Molecule-molecule interactions

For nitrogen the X1 model of Murthy *et al.*[14] is supplemented by the McLachlan substrate-mediated interaction[13] and Steele's model of the nitrogen-graphite interaction.[15] This combination was used in our previous work;[1,4] it gives a good account of a range of date for condensed nitrogen and the results for the monolayer are similar[4] to those for the more recent Etters model.[5] The charge distribution of the molecule is represented by three-point charges located at the atomic and molecular centers; there is an effective quadrupole moment of -1.173×10^{-26} esu cm^2.

For carbon monoxide the basic model is that constructed by Belak, Kobashi, and Etters,[8] who emphasized the similarities of carbon monoxide and molecular nitrogen and used *ab initio* data for nitrogen. The main difference is in the electrostatic multipoles of CO, which are represented by a set of four distributed point charges. The leading moments are electric dipole moment 0.112×10^{-18} esu cm, directed from C to O, and quadrupole moment -1.95×10^{-26} esu cm^2, taken with respect to the center of mass. We include the McLachlan terms[13] with the coefficients given by Belak, Kobashi, and Etters.[8]

2. Molecule-substrate interactions

As for inert gases adsorbed on graphite,[3] there are indications[10] that the corrugation of the molecule-substrate potential formed from isotropic atom-atom potentials is too small; the anisotropy terms of Carlos and Cole[11] have been added to the nitrogen model.[10] Two coefficients γ_A and γ_R specify the modifications to the van der Waals attraction and the overlap repulsion. The value $\gamma_A=0.4$ is set by the dielectric properties of the graphite[11] and γ_R is an adjustable parameter. Carlos and Cole[11] fitted $\gamma_R=-0.54$ for helium; this value may also apply for the other inert gases.[3] Joshi and Tildesley[10] fitted $\gamma_R=-1.05$ for nitrogen. A nitrogen model with the anisotropy terms has a larger zone-center frequency gap than with $\gamma_A=\gamma_R=0$, but it is still only half of the observed value.[1] Anisotropy terms are not yet included in the carbon monoxide model, in view of the large uncertainties in modeling the electrostatic screening of the graphite.

Vernov and Steele[6] propose that bonding in the graphite gives rise to aspherical atomic charge distributions which are the source of electrostatic fields with rapid spatial variation external to the graphite. Specifically, they represent the sources of the fields by axially symmetric quadrupole moments $\Theta_{VS}=-1.3\times10^{-26}$ esu cm^2 at the carbon sites. This value is an average of the quadrupole moment per carbon atom in three aromatic molecules (benzene, naphthalene, and anthracene) with sp^2 bonding. Another source of information is the analysis of x-ray-diffraction intensities for bulk graphite.[12] The resulting valence charge density has a quadrupolar distortion which corresponds to $\Theta=0.4\times10^{-26}$ esu cm^2; when higher multipole terms[12] are included, the effective coefficient for calculating the external electrostatic field is $\Theta_{ex}=1.0\times10^{-26}$ esu cm^2.

A frequent approximation[4,13] to the electrostatic response of the graphite to external charges and permanent moments is to use a screening of the fields de-

scribed by image charges located with respect to a mirror plane at one-half graphite interplanar spacing above the substrate surface atoms. Then the image terms in the energy cause small shifts in the results for the nitrogen monolayer. However, as noted by Belak, Kobashi, and Etters[8] and by Peters and Klein,[9] the effects for the carbon monoxide layer are so large as to cast serious doubt on the procedure. Belak, Kobashi, and Etters[8] found that using point multipoles rather than distributed charges for the screening response for CO on graphite stabilized the calculations. We have examined the origin of the differences in the N_2 and CO cases and find that the CO case is stabilized and the N_2 case changed little if the mirror plane is slightly displaced towards the graphite surface; further details of this argument are given in Appendix B. We adopt a displacement of 0.25 Å: The precise value is not well determined by the argument, but it is similar in magnitude (although opposite in sign) to the shifts adopted[16] for metal surfaces.

The considerable uncertainties in the screening response and the sources of the external electrostatic field may be reduced with extensions of electronic structure calculations for graphite. There is some support[17] for the bulk valence charge densities of the x-ray analysis, while the charge densities at the graphite surface enter in the theory of its behavior in a scanning tunneling microscope.[18] The inward shift proposed for the mirror plane might be tested in a version of the core-level shift experiment used for inert gases on metals.[19]

B. Structures

We treat orientationally ordered monolayer solids with two molecules in a $\sqrt{3}\times 3$ unit cell commensurate with the graphite. The structure is a generalization of the $(\sqrt{3}\times\sqrt{3})R30°$ lattice of molecular centers of mass. The coordinate axes are indicated in Fig. 1: The origin of coordinates is at the center of a surface carbon hexagon and the x axis is oriented perpendicular to a hexagon side. The center of the hexagon is termed a center site C, the midpoint of a hexagon side a bridge site B, and a hexagon vertex an atop site A.

Coordinates for the lattice configurations are the locations of the midpoint (center) of the diatomic molecule [identical with the center of mass (c.m.) for N_2 but not for CO] and angles for the molecular orientations. Lateral positions of the molecules are specified by a vector (X_c, Y_c) which is linearly related to the c.m. of the unit cell and a relative displacement (D_x, D_y) of the molecules from separations in the uniform lattice. Thus, the coordinates of the centers of the two molecules in the unit cell are

$$\begin{aligned}(X_c^{(1)}, Y_c^{(1)}, Z_c^{(1)}) &= (X_c - D_x/2, Y_c - D_y/2, z_1)\ , \\ (X_c^{(2)}, Y_c^{(2)}, Z_c^{(2)}) &= (X_c + 3L/2 + D_x/2, \\ &\qquad Y_c + \sqrt{3}L/2 + D_y/2, z_2)\ ,\end{aligned} \tag{2.1}$$

where $L = 2.46$ Å is the side of a graphite surface unit cell. The orientations of the molecular axes are specified by

$$\hat{\mathbf{n}} = (\cos\phi\cos\chi,\ \cos\phi\sin\chi,\ \sin\phi)\ . \tag{2.2}$$

The general configuration has angles (ϕ_1, χ_1) and (ϕ_2, χ_2). For CO, $\hat{\mathbf{n}}$ is directed from C to O.

The two-in herringbone configurations of our previous work[1,4] have $X_c = Y_c = D_x = D_y = \phi_1 = \phi_2 = 0$ and $\chi_2 = -\chi_1$. In the case of nitrogen, for $Y_c = 0$ and $X_c \neq 0$ the two molecules are in equivalent surface environments for $\chi_1 = -\chi_2$ and $\phi_1 = \phi_2$, while for $X_c = 0$ and $Y_c \neq 0$ the latter relation is changed to $\phi_1 = -\phi_2$. However, if the c.m. variable is displaced from (0,0) molecule-graphite forces drive nonzero values of (D_x, D_y). In view of the absence of two-out ($\phi \neq 0$) monolayer herringbone configurations in earlier calculations[4,9] for nitrogen, it is interesting that models with the Vernov-Steele value[6] of substrate quadrupole have energy minima with $\phi \neq 0$ and nonzero (X_c, Y_c) and (D_x, D_y). Such configurations were obtained also by Belak, Kobashi, and Etters[8] for the commensurate CO on graphite monolayer.

The optimized configuration at the potential-energy minimum retains some symmetries. In the N_2 monolayer

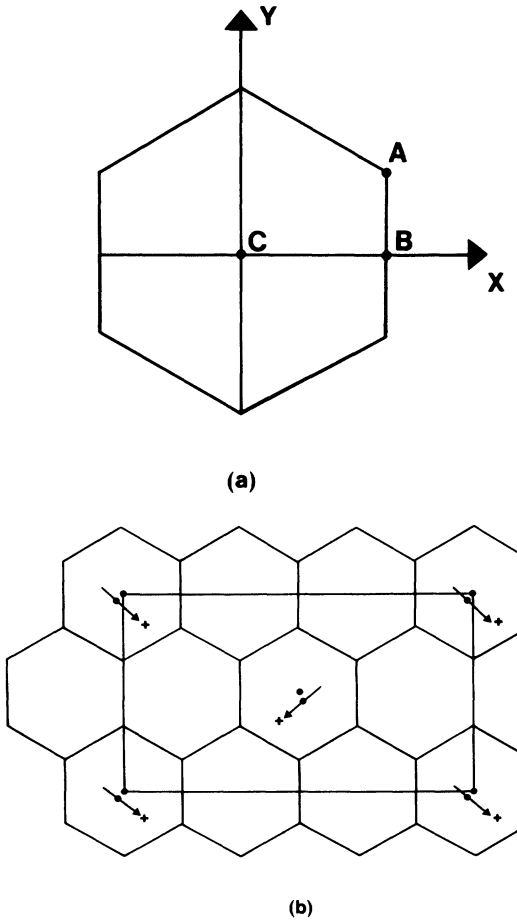

FIG. 1. Schematic of structures on the graphite basal plane surface. (a) Surface carbon hexagon, with x and y coordinate axes and center (C), bridge (B), and atop (A) sites identified. (b) $\sqrt{3}\times 3$ herringbone unit cell, with molecules in the positions of the generalized two-out herringbone found for case CO3 (3,2) of CO on graphite.

solid, the potential-energy minimum has (X_c, Y_c) located (i) on the x axis, (ii) on the y axis, or (iii) at the origin (0,0), depending on the model parameters. The symmetries are then (i) $D_x=0$, $\chi_1=-\chi_2$ and $\phi_1=\phi_2$; (ii) $D_y=0$, $\chi_1=-\chi_2$, and $\phi_1=-\phi_2$; and (iii) $D_x=D_y=\phi_1=\phi_2=0$ and $\chi_1=-\chi_2$. In the CO monolayer solid, the energy minimum has (X_c, Y_c) located on the y axis, with $D_y=0$, $\chi_2=180°-\chi_1$, and $\phi_1=\phi_2$. The latter symmetry is also present in the results of Belak, Kobashi, and Etters for CO on graphite.[8] The minimum-energy configurations for (X_c, Y_c) on either the x or y axes are called generalized herringbone lattices.

The configuration of one molecule, for calculations of the molecule-graphite potential energy, is specified by the position (x,y,z) of its center and the orientation $\hat{\mathbf{n}}$ of its axis.

C. Calculations

Static potential-energy surfaces, for the minimum energy as a function of (x,y) for one molecule and as a function of (X_c, Y_c) for the monolayer solid, are constructed by optimizing the remaining variables. The result gives the minimum barrier to motion on the surface for one adsorbed molecule and for the slipping of the monolayer solid and includes the effects of variations of overlayer height on the minimum-energy lateral motions. The search in three variables for one molecule is performed by adapting parabolic search methods[4] or by applying a more general library routine.[20] The search in eight variables for the monolayer solid is done with the latter method. For N_2 there are no artifacts apparent in the optimized configurations, but for CO the search must be guided by narrowing variable ranges for it to converge to the minimum-energy configuration. Examples of the minimum potential-energy surfaces for the monolayer solid are shown in Fig. 2.

Lattice-dynamics calculations[4] were performed for the two-in herringbone lattices and for special cases $(D_x=D_y=0)$ of the two-out herringbone. Dynamical instabilities in the latter cases led us to consider more general configurations with nonzero D_x and D_y. Minimum quasiharmonic free-energy configurations are determined for two-in herringbone lattices. Then a powder pattern average of the spectral density for an inelastic neutron-scattering experiment is formed.[1]

Minimum frequencies of the commensurate monolayers are also estimated with the Born-Oppenheimer approximation described in Appendix A. These are the only estimates now available for the CO monolayer, in the absence of lattice-dynamics calculations for the generalized herringbone lattice.

The molecule-molecule interactions are truncated for center-of-mass separations larger than 10 Å. Steele's Fourier decomposition[15] is used for the molecule-substrate potential energy and amplitudes for the first two shells of reciprocal-lattice vectors are retained in many of the potential-energy calculations. The contribution of the second shell is quite small (less than 0.5 K/mol) at values of z_1 and z_2 near the potential-energy minimum; it is omitted from the lattice-dynamics calculations. Image energy terms arising from the graphite screening response are omitted from the lattice-dynamics work, but are included in some of the potential-energy calculations.

III. MODELING OF N_2/GRAPHITE

Variants of the basic interaction model,[4] a combination of the X1 model[14] and Steele's parameters[15] for the van der Waals interaction with the substrate, are constructed by choices of the anisotropy parameters and of the graphite quadrupole moment. We present results for several cases to demonstrate the many possibilities which arise even for a herringbone lattice of homonuclear diatomic

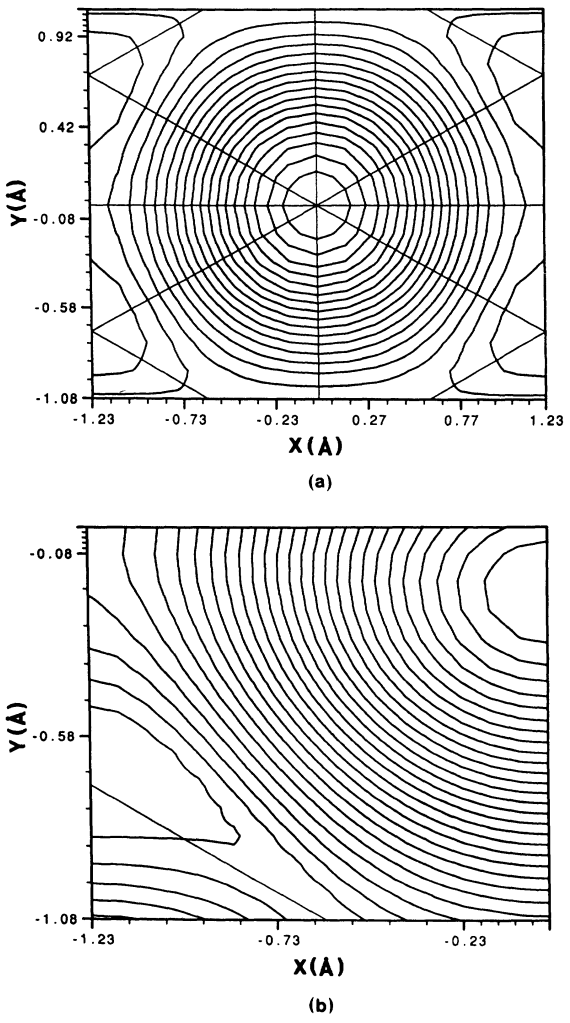

FIG. 2. Contour map of the minimum potential-energy surface of the $\sqrt{3}\times3$ herringbone monolayer solid as a function of the coordinates (X_c, Y_c). (a) Result for case N2F (3,1) of the N_2 on graphite calculations, showing two mirror plane symmetries. The potential-energy minimum is at (0,0) and the spacing between contour levels is 2.4 K. (b) Result for case CO3 (3,2) of the CO on graphite calculations corresponding to one quadrant of (a). The potential-energy minimum is at $(0,-0.18$ Å) and the spacing between contour levels is 0.94 K. The straight lines show the x and y axes, the 30° lines through the center and parts of the basic hexagon of the graphite surface [cf. Fig. 1(a)].

molecules. However, some of these are excluded as plausible models for N_2 on graphite because properties of the minimum-energy lattice are in serious disagreement with salient features of experimental data: The $\sqrt{3}\times 3$ commensurate lattice of N_2 on graphite is a two-in herringbone lattice[21] with a zone-center frequency gap of ca. 0.4 THz ($=1.6$ meV$=20$ K).[1,2]

Designations for several parameter sets are given in Table I. Case N2B was used[4] for a study of monolayer and bilayer structures. Case N2C then incorporates[1] the substrate anisotropy parameters of Joshi and Tildesley[10] and case N2A incorporates the Vernov-Steele quadrupole parameter[6] Θ_{VS}. Case N2D adds the quadrupole parameter Θ_{ex} derived from the x-ray valence charge densities[12] to case N2C. Case N2E is the set used by Vernov and Steele.[6] Case N2F is a combination of inert-gas anisotropy parameters[3,11] and Θ_{ex}. Case N2G is a set which arose in our searches and for which we have many results. Although cases N2A, N2B, N2C, and N2E are excluded as realistic models by data for N_2 on graphite, they are included here because they display interesting effects of the competing terms in the models.

A. One molecule

It is not automatic that the center-of-mass position of minimum potential energy for a single adsorbed homonuclear diatomic molecule is a high symmetry point of the graphite unit cell. This is demonstrated by the results in Table I for cases N2A and N2C. The displacement from the center site for case N2C was noted already by Joshi and Tildesley.[10]

Energy differences between the bridge and center sites and between the atop and center sites are presented in Table I to provide measurements of the topography of the minimum potential energy surface. Case N2E is remarkable in this light for the small difference between the center and atop sites. Vernov and Steele calculated the N_2-graphite potential for cases N2E and N2B: Their values for the potential are close to ours, with small differences which may arise from the modeling of the charge distribution of the N_2 molecule.

Joshi and Tildesley[10] adopted the anisotropy parameters of case N2C, in place of those of cases N2B and N2F, to make the calculated melting temperature of submonolayer commensurate N_2 on graphite be close to the experimental value. They suggested that the significant effect for the melting is that the anisotropy terms increase the barriers to lateral motion. The values for case N2F are relevant in that context: use of the inert-gas anisotropy parameters and Θ_{ex} gives a difference $E(A)-E(C)$ which is much the same as for their parameter set.

The results for the minimum-energy site of one molecule do not directly carry over to the monolayer solid because molecule-molecule interactions cause the molecular orientations to differ from the optimal directions for a single molecule. Indeed, at the center and bridge sites, C and B, the optimal angles ϕ and χ are zero, while for the herringbone lattice the angle χ is ca. 45°.

TABLE I. Parameters and properties of one molecule interacting with the basal plane surface of graphite. Anisotropy parameters as defined by Carlos and Cole (Ref. 11); quadropole moment Θ in units of 10^{-26} esu cm^2 and energies in K; results with two shells of reciprocal-lattice vectors in the Steele Fourier decomposition. The first line of each case has results without substrate screening (image) terms; the second line results with substrate screening approximated by a mirror-image plane at one-half bulk interplanar spacing above the surface plane of carbon atoms.

Label	γ_A	γ_R	Θ	Site[a]	$E(B)-E(C)$	$E(A)-E(C)$	$E(\text{site})-E(C)$
N2A	0.4	−1.05	−1.3	(0.74,0)	−10.0	22.5	−12.9
				(0.72,0)	−10.1	25.4	−13.8
N2B	0.0	0.0	0.0	C	6.9	19.8	0.0
				C	7.6	21.9	0.0
N2C	0.4	−1.05	0.0	(0.27,0)	14.5	40.5	−0.3
				(0.30,0)	16.0	44.5	−0.5
N2D	0.4	−1.05	1.0	C	33.4	54.5	0.0
				C	36.1	59.4	0.0
N2E	0.0	0.0	−1.3	B	−16.8	2.3	−16.7
				B	−17.5	3.4	−17.5
N2F	0.4	−0.54	1.0	C	29.9	46.0	0.0
				C	32.3	50.0	0.0
N2G	0.4	−1.05	1.3	C	39.0	58.7	0.0
				C	42.1	63.8	0.0

[a]Center-of-mass position of minimum potential energy, using the site labels and coordinate system of Fig. 1. C, B, and A denote the center, bridge, and atop sites; (x,y) denotes the Cartesian components (in Å) for more general positions.

B. Commensurate monolayer solid

Properties of the minimum potential-energy configurations for several parameter sets and various approximations for the screening effects of the graphite are listed in Table II. A contour map of the minimum potential-energy surface for case N2F[1,3] is shown in Fig. 2(a).

For cases N2A and N2E, the configurations are two-out herringbone lattices; not only are the molecules tipped with respect to the plane but there is a relative displacement within the cell. For case N2A the tip is about 4° and D_y is about -0.05 Å; for case N2E, ϕ_1 is about $-3°$ and D_x is about 0.04 Å. Diehl and Fain[21] conclude that any tips consistent with their observations must be less than 2°. Also, we estimate that the zone-center gap in these cases is much less than 10 K and thus exclude them as plausible N_2 on graphite models on two grounds.[1,21] However, they are instructive in showing (i) how the generalized herringbone lattice arises after a modification of previous models,[1] and (ii) that the use[6] of Θ_{VS} leads to a frustrated set of interactions and a small corrugation of the energy surface.

Vernov and Steele showed for a single molecule on graphite, in case N2E, that the position of the lowest energy shifted from the hexagon center (C) to the bridge site (B) and that the difference between maximum and minimum energies on the minimum potential-energy surface doubled from its value for case N2B. However, the monolayer lattice for case N2E has a smaller effective corrugation than for case N2B. The orientation which minimizes the single molecule energy is very different from that for the lattice. The van der Waals and electrostatic contributions to the effective corrugation act in a mutually frustrating fashion. This frustration is shown not only in the limited range of energies on the minimum potential-energy surface, but by rapid changes in the local curvatures of the surfaces for cases N2A and N2E as the position (X_c, Y_c) varies.

To discriminate among the other cases in Table II we calculate the two lower frequencies at zero wave vector. The curvatures derived in the potential-energy minimization, V_{xx} and V_{yy}, are used to estimate the frequencies with the Born-Oppenheimer (BO) approximation outlined in Appendix A:

$$\omega_\alpha(\mathrm{BO}) = (V_{\alpha\alpha}/M)^{1/2} . \tag{3.1}$$

The results are listed in Table III, with values from lattice-dynamics calculations performed at the same configuration. The estimate from Eq. (3.1) agrees with the quasiharmonic lattice frequency to better than 5%.

TABLE II. Properties of the minimum potential-energy configuration of the $\sqrt{3}\times 3$ herringbone solid of N_2 on graphite. Labels and sites identified as in Table I; energies in K, curvatures V_{xx} and V_{yy} in K/Å^2. The site label (x',y') gives (X_c, Y_c) of Eq. (2.1) in Å.

Label	Index[a]	Site	Energy	V_{xx}	V_{yy}	$E(B)-E(C)$
N2A	1,2	(0.23,0)	−1480	49	14	22[b]
	2,1	(0.24,0)	−1464	45	15	20[b]
	3,2	(0.22,0)	−1478	27	12	21[b]
N2B	1,2	C	−1477	52	49	19
	2,2	C	−1461	49	46	17
	2,1	C	−1461	47	46	17
N2C	2,1	C	−1475	71	76	35
N2D	1,2	C	−1502	151	148	51
	2,1	C	−1485	135	137	48
N2E	2,1	(0,0.57)	−1451	2	19	2[c]
N2F	1,2	C	−1496	136	132	43
	2,2	C	−1479	128	125	50
	3,2	C	−1494	130	127	42
N2G	1,2	C	−1506	170	167	55
	2,1	C	−1488	153	154	51
	3,2	C	−1503	165	161	53

[a]The index i,j specifies options on the inclusion of substrate screening and on the number of shells retained in the Steele Fourier decomposition of the molecule-substrate potential. The values $i=1$, 2, and 3 denote screening terms with the nondisplaced mirror plane, no screening terms, and screening with the 0.25-Å displacement of the mirror plane, respectively. The values $j=1$ and 2 denote cases with one and two shells of Fourier components, respectively.

[b]$E(C)-E(\min)<0.2$ K.

[c]$E(C)-E(\min)=1.3$ K.

TABLE III. Minimum frequencies at zero wave vector. Minimum frequencies in K at zero wave vector for x and y polarizations, calculated with Eq. (3.1) (BO) and with quasiharmonic lattice dynamics at the configuration of minimum potential enegy.

Label	Index	ω_x(BO)	ω_x(QH)	ω_y(BO)	ω_y (QH)
N2B	2,1	9.0	8.9	8.8	8.8
N2C	2,1	11.0	10.7	11.5	11.3
N2D	2,1	15.2	15.1	15.4	15.3
N2F	2,1	14.6	14.5	14.5	14.5
N2G	2,1	16.2	16.2	16.3	16.3
	1,2	17.1	b	16.9	a
	3,2	16.9	b	16.7	a

[a]No lattice-dynamics calculation.

The positive Θ cases have much larger zone-center gaps than the Joshi-Tildesley model[10] (case C), but the gap is not sensitive to the difference in γ_R from the inert-gas value[3,11] $\gamma_R = -0.54$ (compare D and F). The entries for case G suggest that including image energy terms in the lattice dynamics may increase the calculated zone-center gap by 10%.

In Fig. 3 we show the calculated spectral density[1] for inelastic neutron scattering. The spectra are calculated at configurations which minimize the zero-temperature quasiharmonic free energy.[4] These differ from the minimum potential-energy configurations mainly by an increase of the overlayer height by 0.06 Å, which is accompanied by a lowering of the minimum frequency by 10%. The spectra are spherical powder averages at 4 K for neutrons of final energy 5.04 meV and momentum transfer 1.70 $Å^{-1}$, convoluted with an experimental instrumental resolution function.[1]

The effect of the quadrupole moment in increasing the zone-center gap, with little change in the spectral density at higher frequencies, is shown in Fig. 3(a). Using the value $\gamma_R = -0.54$, fitted for helium, does not change the spectral density appreciably: In Fig. 3(b), the successive curves have $\Theta = 0, 1, 2$ and common values $\gamma_A = 0.4$ and $\gamma_R = -0.54$. Indeed, there are only very small differences apparent when pairs of curves for $\gamma_R = -0.54$ and -1.05 are superposed.

Fields from aspherical atomic charge distributions in the graphite, characterized by the quadrupole moment Θ_{ex} derived from x-ray-diffraction data for bulk graphite,[12] have the effect of markedly narrowing the discrepancy between the calculated[1,3] and measured[1,2] zone-center frequency gap. The remaining discrepancy is ca. 25% and effects at the 10% level from processes such as screening terms and hybridization with substrate modes may narrow it further. However, the dominant contributions to the electrostatic field at the adsorbed molecule come from atoms in the outermost layer of the graphite. There is little information on how the charge distribution at the graphite surface relaxes relative to that in the bulk. We believe that the comparisons to the neutron-scattering data indicate that the effective moment is in the range of that determined[12] for the bulk and that it is opposite in sign to that derived[6] from analysis of a series of aromatic molecules.

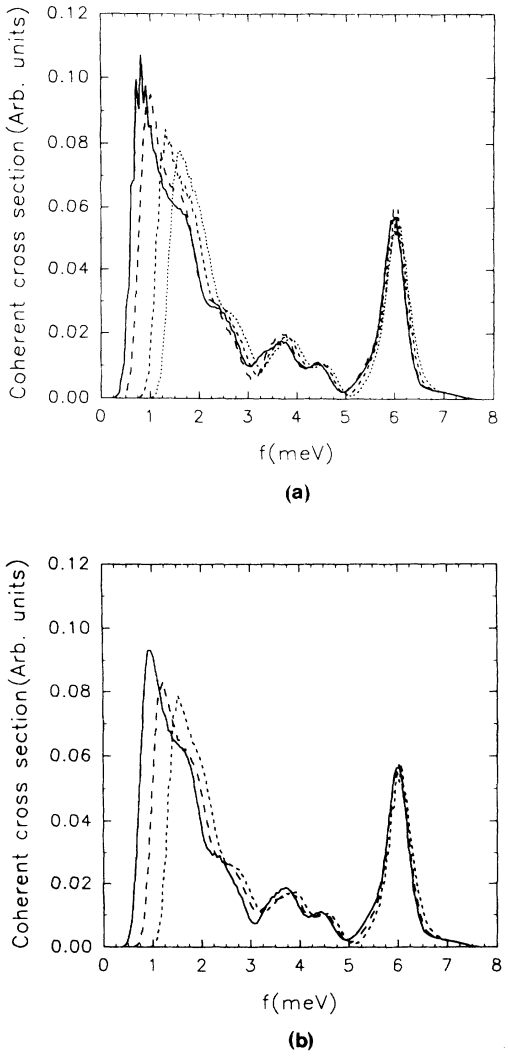

FIG. 3. Spectral density of inelastic neutron scattering from the $\sqrt{3}\times 3$ herringbone lattice of N_2 on graphite. Spherical powder averages at 4 K with final neutron energy 5.04 meV and momentum transfer 1.70 $Å^{-1}$, as in Ref. 1. (a) Cases N2B, N2C, and N2D of Table I, with an additional case N2D′ having $\Theta = 2$ (solid and successively shorter dashed lines, respectively). (b) Three cases based on case N2F of Table I, with $\Theta = 0$, 1, and 2, respectively, for the solid and successively shorter dashed lines.

IV. MODELING OF CO/GRAPHITE

The calculations for CO on graphite are less extensive than for N_2 on graphite; a summary of results is presented in Table IV. The main goal is to test whether the model calculations for CO on graphite discriminate as firmly between the choices of sign for the effective substrate moment as the calculations for N_2 on graphite did. Second, Belak, Kobashi, and Etters[8] introduced an *ad hoc* multiplying factor (*FVG* in Table IV) for the first Fourier amplitude of the CO-graphite potential in order to stabilize the $\sqrt{3}\times 3$ herringbone lattice against incommensurate and pinwheel lattices. We test whether this increase can be achieved with the substrate electrostatic field effects. The calculations are for a monolayer solid with end-to-end ordering[22] of the CO molecules. The samples used in previous diffraction experiments apparently have end-to-end disorder,[23,24] so that the relation of the calculations to the experiments is indirect.

The minimum potential-energy surfaces are more complex than those which arise for N_2 on graphite. The curvatures V_{xx} and V_{yy} at the potential minimum and the energy differences between the minimum and the center site, and between the bridge and center sites, are partial measures of the corrugation potential for the monolayer solid. Values are shown in Table IV for variants of the model of Belah, Kobashi, and Etters, including cases with substrate electrostatic fields. Note that these fields, which were invoked to adjust the frequency spectrum of N_2 on graphite, do not introduce instabilities in the calculations for CO on graphite, a system with larger moments than N_2 on graphite. One quadrant of the surface for case CO3 with index (3,2) is shown in Fig. 2(b); the full surface can be constructed by reflections in the x and y axes.

Modeling of CO on graphite has been troubled[8,9] by apparent instabilities arising in approximations for the substrate screening of fields arising from moments of the CO. The adjustment described in Appendix B reduces that problem. We compare results for the $\sqrt{3}\times 3$ herringbone with and without the adjusted screening terms. Bojan and Steele[25] interpreted their gas-surface virial data for CO on graphite as showing the existence of large electrostatic screening terms, but they did not give an interaction model which included them explicitly.

Cases CO1 and CO2 in Table IV correspond to cases treated by Belak, Kobashi, and Etters[8] and the results for index (2,2) agree with theirs. Their method of treating the substrate screening lowers the energy by 50 K relative to these values; our method gives a lowering of 20 K. The electrostatic energies are indeed much larger for the CO system than for the N_2 system. The 20 K lowering is the net sum of a negative energy ca. 45 K from the electrostatic image energy of one molecule with the graphite, a positive energy ca. 20 K from the static screening charges, and a change in the McLachlan energy, which also depended on the mirror plane location. The curvatures and energy differences on the surface, for a given model in Table IV, are affected little by including substrate screening according to our approximation.

Case CO3 corresponds to the adjustment of the N_2 on graphite model recommended in Sec. III: augment the van der Waals terms in the corrugation with terms arising from the substrate electrostatic fields, calculated us-

TABLE IV. Properties of the minimum potential-energy configuration of the $\sqrt{3}\times 3$ herringbone solid of CO on graphite. Identifications and units as in Tables I and II; *FVG* is a scale factor introduced by Belak, Kobashi, and Etters (Ref. 8) for the first Fourier amplitude of the CO on graphite potential. Sites $(0,y)$ and $(0,-y)$ have equal energy and curvatures.

Label	*FVG*	Θ	Index	Site	E(min)	V_{xx}	V_{yy}	$E(B)-E(C)$	$E(C)-E$(min)
CO1[a]	1	0	2,2	(0,0.02)	−1465	42	46	15	0.1
			3,2	(0,0.06)	−1485	43	48	16	0.1
CO2[a]	2	0	2,2	(0,0.10)	−1478	65	89	31	0.4
			3,2	(0,0.09)	−1499	58	88	32	0.3
CO3	1	1	2,2	(0,0.17)	−1472	63	90	20	1.3
			3,2	(0,0.17)	−1493	67	97	21	1.5
CO3′	1	−1	2,2	(0,0.51)	−1466	62	51	10	6.1
			3,2	(0,0.50)	−1486	65	52	11	6.2
CO4	2	2	2,2	(0,0.25)	−1516	242	364	55	10.9
			3,2	(0,0.25)	−1542	290	425	60	12.7
CO5	2	−2	2,2	(0,0.66)	−1496	199	161	14	36.0
			3,2	(0,0.65)	−1517	210	162	14	37.1
CO6	2	−1	2,2	(0,0.48)	−1482	136	130	22	14.0
CO7	2	1	2,2	(0,0.19)	−1493	112	201	42	3.4

[a]Case *B* of Belak, Kobashi, and Etters (Ref. 8) corresponds to Θ=0 and index (2,1). Their E_1 (Steele) and E_1(CV) subcases correspond to *FVG* = 1 and *FVG* = 2. Differences between results for index (2,1) and (2,2) are very small.

ing Θ_{ex} derived from x-ray data. It has an energy difference $E(B)-E(\min)$ of 22 K, which is intermediate between the values 16 and 32 K for cases CO1 and CO2, respectively. The curvatures at the minimum are quite similar to those for the *ad hoc* adjustment, case CO2. It appears that much of the increase in corrugation required to stabilize the commensurate lattice has the same origin as for N_2 on graphite. Case CO3′ is included to demonstrate that these calculations for CO on graphite do not discriminate as firmly between choice for the sign of Θ as did those for N_2 on graphite. Cases CO4 to CO7 are included to show the effect of larger values of Θ; the positive Θ case has distinctly larger curvature at the minimum-energy configuration.

Of the parameter sets which we have treated, the case CO3 has a corrugation of the minimum potential-energy surface which appears to be large enough to stabilize the commensurate lattice and which is based on a recognized physical mechanism. Anisotropy terms for the van der Waals energies, as used for N_2 on graphite, would increase the corrugation also. For case CO2, found explicitly by Belak, Kobashi, and Etters[8] to stabilize the commensurate lattice, and for case CO3, the zone-center frequency gap is ca. 10 K, using Eq. (3.1).

V. CONCLUDING REMARKS

Electrostatic fields[6] which arise from aspherical charge distributions at atomic sites in a graphite substrate may account for a discrepancy[1] between the calculated and measured values of the Brillouin zone-center frequency gap for the $\sqrt{3}\times3$ herringbone monolayer of N_2 on graphite. Indeed, use of substrate moments derived from bulk valence charge densities in the graphite[12] greatly reduces the discrepancy. The argument is incomplete, because the dominant contributions to the fields arise from atoms in the top plane of the graphite, where there may be some relaxation of the charge density relative to that in the bulk. The present situation is that substrate anisotropy parameters, fitted[11,3] for inert gases, apparently carry over to the interactions for adsorbed molecules and that the spatially varying substrate electric field acts on the molecular moments to increase the corrugation energy. A combination of van der Waals terms and the electrostatic moment energies, with the parameters used here, accounts for most of the observed corrugation in N_2 on graphite. The substrate field term increases the zone-center frequency gap, but has little effect in the spectral density at intermediate and higher frequencies; that part of the spectrum already agreed with the data.[1]

We propose that the cases N2F for N_2 on graphite and CO3 for CO on graphite give a good enough account of present information on the physical systems to merit further study. The nitrogen case incorporates substrate anisotropy effects, by using systematics established for the inert-gas series. Both cases incorporate substrate electrostatic field terms which have a strength based on experimentally determined valence charge densities.

Electrostatic energies are a larger contribution in the CO on graphite monolayer. We have proposed an adjustment to the prescription for the electrostatic screening response of the graphite which stabilizes the calculations for CO on graphite; the substrate fields introduced for N_2 on graphite account for much of the corrugation energy needed for the $\sqrt{3}\times3$ herringbone lattice to be the ground state of CO on graphite. Improved knowledge of the charge density at the graphite surface would help test the validity of the adjustment.

The two-out herringbone configuration, in our calculations, has an associated deformation of the unit cell which is a relative displacement of the molecular centers on the two sublattices. This occurs for a few of our parameter sets for N_2 on graphite, which also have zone-center gaps much less than the experimental value. However, it arises as the minimum potential-energy configuration in each of our calculations for commensurate CO on graphite, in agreement with the results of Belak, Kobashi, and Etters.[8]

It seems inescapable that the substrate electrostatic effects must be included if the discrepancy between the calculated and observed zone-center gap frequency of N_2 on graphite is to be resolved by adjustment of the interaction model. Details of our treatment of the electrostatic terms in the adsorbed layer need to be tested by using the model for a wider range of conditions. Such tests could include calculations of the temperature dependence of the zone-center gap frequency of N_2 on graphite and of the effect of the substrate field terms on the monolayer melting. Applications to other commensurate monolayer solids of linear molecules with larger moments, such as CO_2, would provide even more severe tests.

ACKNOWLEDGMENTS

L.W.B. thanks the Fysisk-Kemisk Institut for its hospitality during the period of this work and acknowledges partial support by National Science Foundation Grant No. DMR-88-17761 and by the Technical University of Denmark.

APPENDIX A: APPROXIMATION FOR THE CENTER OF MASS OSCILLATIONS

Divide the coordinates of the molecules in a unit cell into the (three) center-of-mass coordinates $\mathbf{R}$ and the remaining (internal) coordinates q_i. For the nitrogen cells of this work, the 10 spatial degrees of freedom are divided into three c.m. coordinates and seven internal coordinates. In the static potential-energy minimizations, the internal coordinates are adjusted to minimize the potential energy per molecule $\Phi(q_i,R_\alpha)$,

$$\partial\Phi/\partial q_i|_{\mathbf{R}}=0\ , \tag{A1}$$

and the resulting potential energy is

$$U(\mathbf{R})=\Phi(q(\mathbf{R}),\mathbf{R})\ . \tag{A2}$$

The Born-Oppenheimer approximation for this problem consists of using the second derivatives

$$U_{\alpha\beta}=\partial^2U/\partial R_\alpha\partial R_\beta \tag{A3}$$

as force constants for the oscillatory motion of the mass M (equal to one molecular mass).

To establish the relation of this approximation to the lattice-dynamics calculations define the following matrices:

$$D_{\alpha\beta}=\partial^2\Phi/\partial R_\alpha\partial R_\beta\ , \tag{A4}$$

$$W_{i\alpha}=\partial^2\Phi/\partial R_\alpha\partial q_i\ , \tag{A5}$$

$$V_{ij}=\partial^2\Phi/\partial q_i\partial q_j\ . \tag{A6}$$

Then the matrix U is given by

$$U_{\alpha\beta}=D_{\alpha\beta}-\sum_{i,j}W_{j\alpha}(V^{-1})_{ji}W_{i\beta}\ . \tag{A7}$$

The normal-mode problem of lattice dynamics, for a kinetic energy

$$K=(M/2)\dot{\mathbf{R}}^2+\sum_{i,j}(m_{ij}/2)\dot{q}_i\dot{q}_j \tag{A8}$$

is expressed in terms only of the c.m. coordinates by

$$M\omega^2R_\alpha=\sum_\beta Q_{\alpha\beta}R_\beta \tag{A9}$$

with

$$Q_{\alpha\beta}=D_{\alpha\beta}-\sum_{i,j}W_{j\alpha}[(V-\omega^2m)^{-1}]_{ji}W_{i\beta}\ . \tag{A10}$$

The Born-Oppenheimer approximation follows from the lattice-dynamics theory if the frequency ω is dropped from the right-hand side of Eq. (A10). In other applications, such an approximation is justified by showing that the frequencies associated with the matrix V are large compared to ω. The force constants for the matrix D of the commensurate physisorbed monolayer are generally smaller than those for the matrix V, which involve relative motions of the molecules. In the present work we use the approximation based on Eq. (A3) for estimates of the lowest frequencies of the commensurate monolayer solids. Lattice-dynamics calculations for many nitrogen cases have lowest frequencies which are given to 10% by Eq. (A3).

APPENDIX B: DISPLACEMENT OF THE ELECTROSTATIC MIRROR PLANE

In potential-energy minimizations for the nitrogen monolayer, the image energies perturb the configuration only slightly if the search range for z_1 and z_2 is held to the range 3.25–3.40 Å. When the range is extended to 1.80–3.40 Å, the image terms dominate in the way reported[8,9] for CO on graphite. This problem arises from using the image screening approximation[13,16] at too small separations; stable results with z's near 3.3 Å presumably are obtained because the potential energy has a barrier against collapse to smaller z's. To verify this picture, we form the potential energy as a function of $z_1=z_2=z$, optimizing the other eight variables: There is a potential barrier of height several thousand kelvins for z near 2.5 Å. By contrast, for CO on graphite with the model of Belak, Kobashi, and Etters[8] and screening using the undisplaced mirror plane,[4,13] the potential energy decreases monotonically as z decreases.

As an *ad hoc* remedy, we displace the mirror plane to smaller distances. The displacement in chosen so that, as z decreases, the potential energy of CO on graphite rises by 1000 K from a minimum near 3.3 Å before it starts to decrease again. The displacement 0.25 Å accomplishes this, and there is a local potential maximum at 2.8 Å. Using the 0.25-Å value in the nitrogen calculations changes the total image energy terms ca. 3 K for z near 3.3 Å. With the original specification of the mirror plane, the image energy for a single N_2 molecule is ca. -30 K and the image energy per molecule in the N_2 herringbone monolayer is ca. -15 K out of a total potential energy of ca. -1500 K/mol. Thus the change required to stabilize the CO on graphite calculations has little effect in the N_2 on graphite case.

We conclude that the larger electrostatic moments for CO cause it to be a marginal case for the nondisplaced mirror plane since a small adjustment stabilizes the calculation. Indeed, Belak, Kobashi, and Etters[8] stabilized their CO calculations with a different small modification. Calculations for CO molecules perpendicular to the surface indicate that the 0.25-Å displacement will also stabilize the screening terms for CO pinwheel structures,[8,9] but we have not treated the pinwheel lattice directly.

[1]F. Y. Hansen, V. L. P. Frank, H. Taub, L. W. Bruch, H. J. Lauter, and J. R. Dennison, Phys. Rev. Lett. **64**, 764 (1990).

[2]H. J. Lauter, V. L. P. Frank, H. Taub, and P. Leiderer, *Proceedings of the 19th International Conference on Low Temperature Physics,* edited by D. S. Betts [Physica B **165&166**, 611 (1990).

[3]L. W. Bruch, in *Phase Transitions in Surface Films 2,* edited by H. Taub, G. Torzo, H. J. Lauter, and S. C. Fain, Jr. (Plenum, New York, 1991).

[4]S. E. Roosevelt and L. W. Bruch, Phys. Rev. B **41**, 12 236 (1990).

[5]B. Kuchta and R. D. Etters, Phys. Rev. B **36**, 3400 (1987); **36**, 3407 (1987).

[6]A. Vernov and W. A. Steele (unpublished).

[7]D. Nicholson, R. F. Cracknell, and N. G. Parsonage, Mol. Simul. **5**, 307 (1990).

[8]J. Belak, K. Kobashi, and R. D. Etters, Surf. Sci. **161**, 390 (1985).

[9]C. Peters and M. L. Klein, Mol. Phys. **54**, 895 (1985).

[10]Y. P. Joshi and D. J. Tildesley, Mol. Phys. **33**, 699 (1985).

[11]W. E. Carlos and M. W. Cole, Surf. Sci. **119**, 21 (1982).

[12]R. Chen, P. Trucano, and R. F. Stewart, Acta Crystallogr. Sect. A **33**, 823 (1977).

[13]L. W. Bruch, Surf. Sci. **125**, 194 (1983).

[14]C. S. Murthy, K. Singer, M. L. Klein, and I. R. McDonald, Mol. Phys. **41**, 1387 (1980).

[15]W. A. Steele, J. Phys. (Paris) Colloq. **38**, C4-61 (1977).

[16]N. D. Lang and W. Kohn, Phys. Rev. B **7**, 3541 (1973);

E. Zaremba and W. Kohn, *ibid.* **13**, 2270 (1976).
[17]N. A. W. Holzwarth, S. G. Louie, and S. Rabii, Phys. Rev. B **26**, 5382 (1982).
[18]I. P. Batra, N. Garcia, H. Rohrer, H. Salemink, E. Stoll, and S. Ciraci, Surf. Sci. **181**, 126 (1987); D. Tomanek and S. G. Louie, Phys. Rev. B **37**, 8327 (1988).
[19]G. Kaindl, T.-C. Chiang, D. E. Eastman, and F. J. Himpsel, Phys. Rev. Lett. **45**, 1808 (1980).
[20]Multiparameter Optimization Code ZXMWD of the IMSL Library.
[21]R. D. Diehl and S. C. Fain, Jr., Surf. Sci. **125**, 116 (1983).
[22]A. Inaba, T. Shirakami, and H. Chihara, Chem. Phys. Lett. **146**, 63 (1988).
[23]H. You and S. C. Fain, Jr., Surf. Sci. **151**, 361 (1985); Phys. Rev. B **34**, 2480 (1986).
[24]K. Morishige, C. Mowforth, and R. K. Thomas, Surf. Sci. **151**, 289 (1985).
[25]M. J. Bojan and W. A. Steele, Langmuir **3**, 116 (1987); **3**, 1123 (1987).